



Looking upstream with clumped and triple oxygen isotopes of estuarine oyster shells in the early Eocene of California, USA

Julia R. Kelson, Sierra V. Petersen, Nathan A. Niemi, Benjamin H. Passey and Allison N. Curley

Department of Earth and Environmental Sciences, University of Michigan, 1100 North University Avenue, Ann Arbor, Michigan 48109, USA

ABSTRACT

The $\delta^{18}\text{O}$ of carbonate minerals that formed at Earth's surface is widely used to investigate paleoclimates and paleo-elevations. However, a multitude of hydrologic processes can affect $\delta^{18}\text{O}$ values, including mixing, evaporation, distillation of parent waters, and carbonate growth temperatures. We combined traditional carbon and oxygen isotope analyses with clumped (Δ_{47}) and triple oxygen isotopes ($\Delta^{17}\text{O}$) analyses in oyster shells (*Acutostrea idriensis*) of the Goler Formation in southern California (USA) to obtain insights into surface temperatures and $\delta^{18}\text{O}$ values of meteoric waters during the early Eocene hothouse climate. The Δ_{47} -derived temperatures ranged from 9 °C to 20 °C. We found a correlation between the $\delta^{18}\text{O}$ of growth water ($\delta^{18}\text{O}_{\text{gw}}$) (calculated using Δ_{47} temperatures and $\delta^{18}\text{O}$ of carbonate) and the $\delta^{13}\text{C}$ values of shells. The $\Delta^{17}\text{O}$ values of shell growth waters (0.006‰–0.013‰ relative to Vienna standard mean ocean water–standard light Antarctic precipitation [VSMOW–SLAP]) calculated from $\Delta^{17}\text{O}$ of carbonate (−0.087‰ to −0.078‰ VSMOW–SLAP) were lower than typical meteoric waters. These isotopic compositions are consistent with oyster habitation in an estuary. We present a new triple oxygen isotope mixing model to estimate the $\delta^{18}\text{O}$ value of freshwater supplying the estuary ($\delta^{18}\text{O}_{\text{fw}}$). The reconstructed $\delta^{18}\text{O}_{\text{fw}}$ of −11.3‰ to −14.7‰ (VSMOW) is significantly lower than the $\delta^{18}\text{O}_{\text{gw}}$ of −4.4‰ to −9.9‰ that would have been calculated using “only” Δ_{47} and $\delta^{18}\text{O}$ values of carbonate. This $\delta^{18}\text{O}_{\text{fw}}$ estimate supports paleogeographic reconstructions of a Paleogene river fed by high-elevation catchments of the paleo-southern Sierra Nevada. Our study highlights the potential for paired Δ_{47} and $\Delta^{17}\text{O}$ analyses to improve reconstructions of meteoric water $\delta^{18}\text{O}$, with implications for understanding ancient climates and elevations.

INTRODUCTION

The climate and topography of mountainous western North America during the hothouse of the early Eocene remain enigmatic because contemporaneous changes in surface temperature, elevation, and hydrologic processes are entangled in the geologic record (Hren et al., 2010; Mix et al., 2016; Ibarra et al., 2021). The $\delta^{18}\text{O}$ of authigenic carbonates is widely used as a proxy for $\delta^{18}\text{O}$ of meteoric waters in reconstructing paleoclimates and paleo-elevation histories. However, even with growth temperature constrained through clumped isotopes (Δ_{47}), $\delta^{18}\text{O}$ of carbonate growth water ($\delta^{18}\text{O}_{\text{gw}}$) is a nonunique recorder of terrestrial environments because it is sensitive to topography and various hydrologic processes (Fig. 1). We show that pairing clumped (Δ_{47}) and triple oxygen isotopes ($\Delta^{17}\text{O}$) improves our ability to disentangle the various factors that affect $\delta^{18}\text{O}_{\text{gw}}$. This approach

promises to improve our understanding of past climates by offering novel constraints on the elevation history of the Cordillera and thus the ability to relate continental and marine climate records to each other and to model predictions (Naafs et al., 2018; Lunt et al., 2021).

Triple oxygen isotopes reveal nonequilibrium processes that cause the relationship between $\delta^{17}\text{O}$ and $\delta^{18}\text{O}$ to deviate from that observed in meteoric waters. The $\Delta^{17}\text{O}$ value is defined as a deviation from a reference slope ($\lambda_{\text{ref}} = 0.528$) based on variation in meteoric waters primarily driven by Rayleigh distillation (Fig. 1; Luz and Barkan, 2010). Distillation of a water mass as it proceeds into a continent and over topography results in progressively lower $\delta^{18}\text{O}$ values but little change in $\Delta^{17}\text{O}$ values (Fig. 1B; Luz and Barkan, 2010). Evaporation, which is common in terrestrial settings, increases $\delta^{18}\text{O}$ and decreases $\Delta^{17}\text{O}$ as they evolve along a slope shallower

than λ_{ref} (e.g., $\theta = 0.5185$ for kinetic diffusion of water vapor; Fig. 1C; Barkan and Luz, 2007). Mixing of isotopically heavy ocean waters and isotopically light riverine waters in an estuarine environment (Fig. 1D) also obscures $\delta^{18}\text{O}_{\text{fw}}$, leading to $\delta^{18}\text{O}$ values preserved in fossil shells that do not map directly onto either freshwater or seawater.

We measured paired Δ_{47} and $\Delta^{17}\text{O}$ values of 10 early Eocene estuarine oyster shells from exposures of the Goler Formation in the El Paso Mountains, eastern California (USA) (from the collections of the Raymond M. Alf Museum of Paleontology, Claremont, California). We found relatively mild local temperatures through Δ_{47} measurements; these temperatures provided a sea-level datum with which to constrain continentality and inland elevations. Further, we used $\Delta^{17}\text{O}$ to unmix $\delta^{18}\text{O}$ of freshwater ($\delta^{18}\text{O}_{\text{fw}}$) supplying the estuary. In doing so, we show that traditional $\delta^{18}\text{O}$ measurements of carbonate, even combined with Δ_{47} temperatures, result in an overestimate of $\delta^{18}\text{O}_{\text{fw}}$ and an underestimate of paleo-elevations compared to those revealed with $\Delta^{17}\text{O}$ in this setting.

MATERIALS AND ASSESSMENT OF PRESERVATION

The Goler Formation is a thick (4 km) section of terrestrial sediments with a thin (18 m) capping marine siltstone (McDougall, 1987; Squires, 2018). The terrestrial sediments record a meandering to braided river that flowed along the east side of the Paleogene Sierra Nevada and turned west to meet the Pacific Ocean (Cox, 1982; Lechler and Niemi, 2011). Detrital zircon provenance indicates that the Goler Formation was sourced from the Sierra Nevada and the western Nevadaplano (Fig. 1; Lechler and Niemi, 2011). The base of the marine siltstone hosts Ypresian (early Eocene) *Acutostrea idriensis* (Squires, 2018) oyster shell fragments (calcitic); this age designation is consistent with

CITATION: Kelson, J.R., et al., 2022, Looking upstream with clumped and triple oxygen isotopes of estuarine oyster shells in the early Eocene of California, USA: *Geology*, v. XX, p. , <https://doi.org/10.1130/G49634.1>

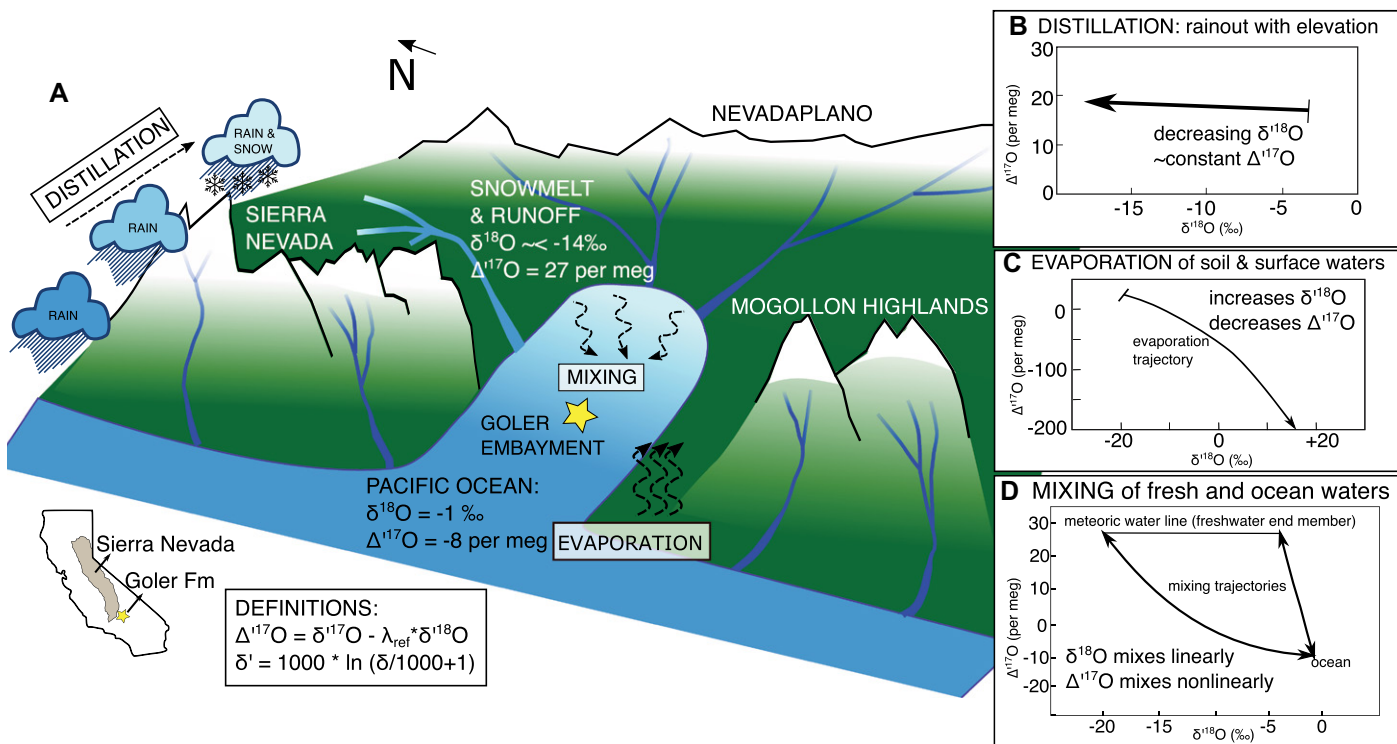


Figure 1. (A) Geographic and landscape position of the Goler Formation (southern California, USA) in the early Eocene and select hydrologic processes relevant to $\delta^{18}\text{O}$ measured in oyster shells. (B) Meteoric water from the Pacific Ocean undergoes Rayleigh distillation as it travels inland and over the Sierra Nevada; rainout decreases $\delta^{18}\text{O}$ but does not change $\Delta^{17}\text{O}$. (C) Evaporation of surface waters lowers $\Delta^{17}\text{O}$ and raises $\delta^{18}\text{O}$ relative to primary precipitation. (D) Isotopically depleted fluvial waters flowed along the east side of the Sierra Nevada and then turned west into the Goler basin (Lechner and Niemi, 2011). Mixing of freshwater and ocean water results in estuarine water with lower $\Delta^{17}\text{O}$ and higher $\delta^{18}\text{O}$ relative to freshwater. Nonlinear mixing in $\Delta^{17}\text{O}$ is due to logarithmic notation in its definition. $\Delta^{17}\text{O}$ values are given in per meg, where 1 per meg = 0.001‰.

magnetostratigraphy and mammalian biostratigraphy (Albright et al., 2010; Lofgren et al., 2014).

The available evidence suggests good preservation of the primary calcite of the oyster shells. Scanning electron microscope (SEM) images show well-preserved textures, minimal dissolution, and no evidence of secondary growth or recrystallization (see the Supplemental Material¹). Solid-state reordering of C-O bonds (thus altering Δ_{47}) is unlikely because the total overburden for the calcitic oyster shells is <2 km (Cox, 1982), implying burial temperatures (<80 °C) that are too low for measurable reordering over time scales corresponding to the age of the samples (56–50 Ma; Hemingway and Henkes, 2021).

STABLE ISOTOPE METHODS

Each one of the 10 oyster shells was analyzed for $\delta^{18}\text{O}$ and $\delta^{13}\text{C}$ in one or two spots to

characterize variability. The Δ_{47} was measured in six shells that spanned the observed range in $\delta^{18}\text{O}$ and $\delta^{13}\text{C}$ values, at the University of Michigan (Ann Arbor, Michigan, USA) (using the methods of Petersen et al. [2016]). Carbonate $\Delta^{17}\text{O}$ measurements were performed on three shells at the University of Michigan using the reduction-fluorination method of Passey et al. [2014]. Growth water isotope values ($\delta^{18}\text{O}_{\text{gw}}$ and $\Delta^{17}\text{O}_{\text{gw}}$) were calculated from measured carbonate values (clumped isotope temperature [$T\Delta_{47}$], $\delta^{18}\text{O}_{\text{carb}}$, and $\Delta^{17}\text{O}_{\text{carb}}$) using relevant fractionation factors (Table 1; see the Supplemental Material; Kim and O’Neil, 1997). Given that the triple oxygen isotope fractionation between carbonate and water is key for reconstructing $\Delta^{17}\text{O}_{\text{gw}}$, we confirmed the triple isotope fractionation exponent in our laboratory (0.5250 ± 0.00007 [1 standard error, SE]) with measurements of modern mollusks and growth waters collected in coastal California and southern Michigan (see the Supplemental Material) and synthetic calcites from Huth et al. (2022).

RESULTS AND INTERPRETATION

Cold Oyster Growth Temperatures from Clumped Isotopes

Measured Δ_{47} values of fossil oyster carbonate ranged from 0.704‰ to 0.739‰ (SE of 0.005‰–0.012‰), corresponding to

temperatures of 9–20 °C (SE of 2–4 °C; Table 1). The range in temperatures likely reflects seasonal variation; Δ_{47} measurements were from bands that likely each record <1 yr of shell growth (i.e., Surge et al., 2001). These Δ_{47} temperatures are among the coldest temperatures reported for the latest Paleocene–early Eocene amongst near-sea-level terrestrial records from western North America, marine records, and climate model predictions (e.g., Yapp, 2008; Mix et al., 2016; Hollis et al., 2019; Zhu et al., 2019). While most modern mollusks preferentially grow during the warm season, hot Eocene summers could have limited oyster productivity at that time (Surge et al., 2001), leading to an overall cool bias in the measured $T\Delta_{47}$. We also might expect estuarine waters to be colder than zonal means as a result of embayment depth and upwelling (Macarewicz et al., 2021), coastal fog (Mix et al., 2016), or contributions of high-elevation runoff. Water temperatures can be as low as ~5 °C in free-flowing rivers once they reach sea level in modern California (e.g., the Mad River; see the Supplemental Material). Regardless of the cause, our data show that cool temperatures persisted locally or seasonally in coastal regions at mid-latitudes (~36°N) during the early Eocene, even as tropical ocean temperatures were elevated. These temperatures can be used to assess continentality and to benchmark temperature-based

¹Supplemental Material. Additional details on the sample preparation, analytical methods, screening for diagenesis and vital effects, carbonate-water triple oxygen isotope fractionation, and the mixing model and code that is used to calculate $\delta^{18}\text{O}_{\text{fw}}$. Please visit <https://doi.org/10.1130/GEOL.S.19386212> to access the supplemental material, and contact editing@geosociety.org with any questions. Supporting clumped isotope data can be found in the EarthChem database: <https://doi.org/10.26022/IEDA/112214>.

TABLE 1. $\Delta^{18}\text{O}$, $\Delta^{13}\text{C}$, Δ_{47} , AND $\Delta^{17}\text{O}$ VALUES OF THE GOLER FORMATION CARBONATES AND GROWTH WATERS

Sample ID	n	Measured values					Calculated values					f_{fw} (± 1 SD from $n = 10,000$)	
		$\delta^{13}\text{C}_{\text{carb}}^*$ (%, VPDB)	$\delta^{18}\text{O}_{\text{carb}}^*$ (%, VPDB)	Δ_{47}^* (± 1 SE)	n	$\delta^{18}\text{O}_{\text{carb}}^{\dagger}$ (%, VSMOW)	$\delta^{18}\text{O}_{\text{carb}}^{\dagger}$ (%, VSMOW)	$\Delta^{17}\text{O}_{\text{carb}}^{\dagger}$ (%, $\lambda_{\text{ref}} = 0.528$)	Temp [§] ($^{\circ}\text{C}$) (± 1 SE)	$\delta^{18}\text{O}_{\text{gw}}^{\#}$ (%, VSMOW)	$\Delta^{17}\text{O}_{\text{gw}}$ VSMOW-SLAP	$\delta^{18}\text{O}_{\text{fw}}$ (%, SD from $n = 10,000$)	
Goler1	4	-1.2 \pm 0.1	-6.9 \pm 0.1	0.707 \pm 0.011	N.A.	N.A.	N.A.	N.A.	19 \pm 4	-5.8 \pm 0.8	N.A.	N.A.	N.A.
Goler2	4	-1.3 \pm 0.1	-7.2 \pm 0.1	0.708 \pm 0.013	N.A.	N.A.	N.A.	N.A.	19 \pm 4	-6.1 \pm 0.8	N.A.	N.A.	N.A.
Goler3	3	-5.5 \pm 0.2	-8.9 \pm 0.1	0.739 \pm 0.005	3	22.190 \pm 1.674	21.948	-0.087 \pm 0.002	9 \pm 2	-9.9 \pm 0.2	0.008	-14.7 \pm 1.6	0.63 \pm 0.10
Goler4	3	-0.6 \pm 0.1	-5.1 \pm 0.2	0.712 \pm 0.006	4	24.004 \pm 0.337	23.721	-0.083 \pm 0.006	17 \pm 2	-4.4 \pm 0.4	0.006	-11.4 \pm 2.8	0.52 \pm 0.15
Goler6a	3	-3.1 \pm 0.1	-8.3 \pm 0.1	0.705 \pm 0.010	N.A.	N.A.	N.A.	N.A.	20 \pm 3	-7.0 \pm 0.6	N.A.	N.A.	N.A.
Goler8b	5	-4.9 \pm 0.4	-9.2 \pm 0.2	0.720 \pm 0.011	3	21.427 \pm 1.471	21.201	-0.078 \pm 0.007	15 \pm 4	-9.0 \pm 0.9	0.013	-12.9 \pm 2.5	0.69 \pm 0.14

Note: VSMOW—Vienna standard mean ocean water; VPDB—Vienna Peepee belemnite; SLAP—standard light Antarctic precipitation.

*Measured in CO_2 evolved from digestion of CaCO_3 in phosphoric acid held at 75°C . Acid fractionation correction (ARFacid) of 0.072 was applied to Δ_{47} values (Petersen et al., 2019). $\delta^{18}\text{O}_{\text{carb}}$ versus Vienna Peepee belemnite (VPDB) was calculated from $\delta^{18}\text{O}$ versus working gas using an empirically derived acid fractionation factor of 1.008122 (established via $\delta^{18}\text{O}$ values measured in standards for Carrera Marble and Ooids, which have established true values relative to NBS 18 and NBS 19 reference materials).

[†]Reported as mineral values via the International Atomic Energy Agency (IAEA) standard IAEA-603 (Wostbrook et al., 2020; Huth et al., 2022). Measured in O_2 evolved from CaCO_3 via acid digestion, reduction, and fluorination (Passey et al., 2014). Error is identical for $\delta^{18}\text{O}$ and $\delta^{18}\text{O}_{\text{carb}}$. N.A.—not analyzed.

[§]Temperature calculated using Petersen et al.'s equation 1 (2019), where $\Delta_{47} = (0.0383 \times 10^6 \times T^2) + 0.258$.

[#]Calculated with the $\delta^{18}\text{O}$ of carbonate analyzed as CO_2 , clumped isotope temperature ($T_{\Delta_{47}}$), and the carbonate-water fractionation of Kim and O'Neil (1997). $\delta^{18}\text{O}_{\text{gw}}$ was calculated versus Vienna standard mean ocean water (VSMOW). Error was propagated from the temperature error (1 SE).

paleo-elevation estimates made in the continental interior (e.g., Lechner et al., 2013; Snell et al., 2014; Ibarra et al., 2021).

Determining Growth Environment and Looking Upstream with Triple Oxygen Isotopes

Our favored explanation for the stable isotopic composition of the oyster shells is that the oysters lived in an estuary, but we also considered the effect of evaporation. The 10 oyster shells had $\delta^{13}\text{C}$ values of -0.5‰ to -6.0‰ (Vienna Peepee belemnite [VPDB]), $\delta^{18}\text{O}_{\text{carb}}$ values of -4.6‰ to -9.5‰ (VPDB), and $\delta^{18}\text{O}_{\text{gw}}$ values of -4.4‰ to -9.9‰ (VSMOW; Table 1). We

calculated $\Delta^{17}\text{O}_{\text{gw}}$ values of 0.006‰ to -0.013‰ (Vienna standard mean ocean water–standard light Antarctic precipitation [VSMOW-SLAP]; SE of carbonate analyses of 0.002‰ to -0.007‰ ; Table 1). These $\Delta^{17}\text{O}_{\text{gw}}$ values are lower than the mean $\Delta^{17}\text{O}$ of meteoric waters in the western United States (0.027‰) and suggest that the oysters were growing in either evaporated freshwater (fw) or a mix of freshwater and ocean water (Fig. 1). From isotopes alone, evaporation could explain the range in $\delta^{18}\text{O}$ and the low $\Delta^{17}\text{O}_{\text{gw}}$ values derived from the oyster shells (Fig. 1C). If we assume that the shells formed in a semiclosed, evaporative body of water, we can estimate $\delta^{18}\text{O}_{\text{fw}}$ with the approach of Passey and

Ji (2019). Using $\Delta^{17}\text{O}_{\text{mw}} = 0.027\text{‰} \pm 0.005\text{‰}$, we calculated $\delta^{18}\text{O}_{\text{fw}}$ values of $-12.4\text{‰} \pm 2.4\text{‰}$ (Goler 4), $-15.6\text{‰} \pm 2.3\text{‰}$ (Goler 3), and $-14.5\text{‰} \pm 3.0\text{‰}$ (Goler 8); these values are significantly lower than the $\delta^{18}\text{O}_{\text{gw}}$ values.

While we cannot rule out the possibility that evaporation affected the oyster growth water, the sedimentologic context supports the idea that the isotopic composition recorded by the shells was dominated by mixing of waters in an estuary. The correlation between $\delta^{13}\text{C}$ and $\delta^{18}\text{O}_{\text{gw}}$ ($r^2 = 0.95$; Fig. 2) and the low $\Delta^{17}\text{O}_{\text{gw}}$ values (relative to precipitation) are consistent with habitation in an estuary where isotopically light freshwater mixed with ocean water (Surge et al.,

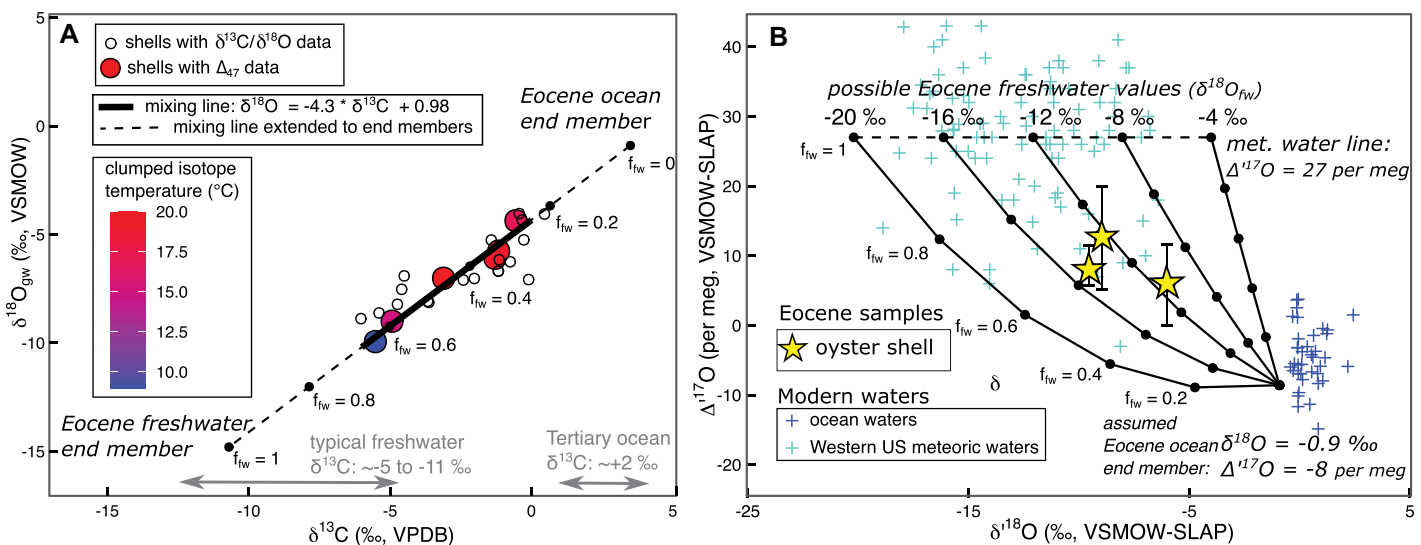


Figure 2. Stable isotope values of Goler Formation (southern California, USA) oysters and mixing models, where f_{fw} is fraction of freshwater. (A) Linear mixing between $\delta^{13}\text{C}$ and $\delta^{18}\text{O}$ of ocean water and freshwater, where $\delta^{18}\text{O}_{\text{gw}}$ was calculated using the clumped isotope temperature ($T_{\Delta_{47}}$) or using the mean $T_{\Delta_{47}}$ (16.5°C) for shells without Δ_{47} data. Regression was made through shells with Δ_{47} data and extended to end members of the ice-free Eocene ocean ($\delta^{18}\text{O} = -0.9\text{‰}$) and $\delta^{18}\text{O}_{\text{fw}}$, derived from $\Delta^{17}\text{O}$ mixing. (B) Triple oxygen isotope mixing between Eocene ocean water and freshwater (fixed $\Delta^{17}\text{O}_{\text{fw}}$; varying $\delta^{18}\text{O}_{\text{fw}}$). Error shown on samples is $\pm 1 \text{ SE}$ (standard error) of replicate analyses of carbonate. Modern waters are shown for illustration (Aron et al., 2021). VSMOW—Vienna standard mean ocean water; VPDB—Vienna Peepee belemnite; SLAP—standard light Antarctic precipitation.

2001; Petersen et al., 2016). We modeled mixing between freshwater and ocean water in triple oxygen isotopes ($\delta^{17}\text{O}$ and $\delta^{18}\text{O}$) to estimate the $\delta^{18}\text{O}_{\text{fw}}$ that fed the Eocene estuary (Fig. 2) using the following equation for ^{17}O and ^{18}O :

$$\delta_{\text{ew}} = \delta_{\text{ow}} \times (1 - f_{\text{fw}}) + \delta_{\text{fw}} \times f_{\text{fw}}, \quad (1)$$

where f_{fw} is the fraction of freshwater (from 0 to 1), δ_{fw} is the incoming freshwater, δ_{ow} is ocean water, and δ_{ew} is estuarine water as recorded by the oyster shells (i.e., $\delta^{18}\text{O}_{\text{gw}}$). This equation was combined with the definition of $\Delta^{17}\text{O}$ and numerically solved for a unique solution of $\delta^{18}\text{O}_{\text{fw}}$ and f_{fw} for each shell (using ratio [R] and δ notation; see the R script in the Supplemental Material). We constrained the parameters through measurements of shell compositions ($\delta^{18}\text{O}$, $\Delta^{17}\text{O}$, $T\Delta_{47}$) from which we derived estuarine water values, estimates for an ice-free ocean ($\delta^{18}\text{O}_{\text{ow}}$ and $\Delta^{17}\text{O}_{\text{ow}}$; see the Supplemental Material), and the assumption of $\Delta^{17}\text{O}_{\text{fw}} = 0.027\text{‰} \pm 0.005\text{‰}$ (Table S1; Aron et al., 2021). Precise constraints on the $\Delta^{17}\text{O}_{\text{fw}}$ in the Eocene do not exist, but the relatively small variability on a global scale suggests that it is reasonable to use the modern western United States value as a baseline (see the Supplemental Material; Passey and Ji, 2019; Ibarra et al., 2021). A Monte-Carlo approach was used to propagate uncertainty in the assumed and measured isotope values and the carbonate-water frac-

tionation factors. We estimated $\delta^{18}\text{O}_{\text{fw}}$ (± 1 SD) values of $-14.7\text{‰} \pm 1.6\text{‰}$, $-11.4\text{‰} \pm 2.8\text{‰}$, and $-12.9\text{‰} \pm 2.5\text{‰}$, corresponding to f_{fw} values of 0.63, 0.52, and 0.69 (Table 1). Mixing in $\delta^{13}\text{C}-\delta^{18}\text{O}_{\text{gw}}$ confirms the plausibility of our estimated $\delta^{18}\text{O}_{\text{fw}}$: when the linear regression through $\delta^{13}\text{C}-\delta^{18}\text{O}_{\text{gw}}$ was extended to the predicted end members for $\delta^{18}\text{O}_{\text{fw}}$ and $\delta^{18}\text{O}_{\text{ow}}$, we predicted $\delta^{13}\text{C}$ values within those expected (Fig. 2; Sackett and Moore, 1966; Veizer et al., 1999).

Low $\delta^{18}\text{O}$ Values of Freshwaters Feeding the Estuary Imply High Elevations Upstream

Both the evaporation and estuarine mixing scenarios provide evidence for isotopically light freshwaters feeding the Goler basin. The low $\delta^{18}\text{O}_{\text{fw}}$ values (minimum of $\sim -14.7\text{‰} \pm 1.6\text{‰}$ from estuarine mixing) suggest that elevated topography existed upstream. A compilation of published $\delta^{18}\text{O}$ data from modern rivers and springs in North America suggest that low-elevation surface waters with $\delta^{18}\text{O}$ of $\sim -14.7\text{‰} \pm 1.6\text{‰}$ exist and likely integrate isotopically lighter water from elevations > 1 km (Fig. 3). Because the $\delta^{18}\text{O}$ value of lowland rivers records a precipitation-weighted hypsometric mean, precise upstream elevations are impossible to discern (Rowley, 2007). Using the approach of Fan and Dettman (2009), we estimated that rivers that drained exclusively low

elevations at the latitudes of the Goler Formation ($\sim 36.5^\circ\text{N}$) in the Eocene would have had a $\delta^{18}\text{O}$ of $\sim -3\text{‰} \pm 3\text{‰}$ —a value that is $\sim 10\%$ higher than the Goler $\delta^{18}\text{O}_{\text{fw}}$ value. Calculating upstream elevations with this $\Delta\delta^{18}\text{O}$ and a typical modern precipitation lapse rate ($\sim 3\text{‰}/\text{km}$; Rowley, 2007) would yield an estimate on the order of $\sim 3\text{--}4$ km elevation. This estimate is consistent with previous estimates of elevations of > 2 km in the central and western Nevada-plano (Snell et al., 2014; Ibarra et al., 2021) and a high-elevation central Sierra Nevada (House et al., 1998). Despite wholesale crustal collapse to sea level at the southernmost tip of the present-day Sierra Nevada (Chapman et al., 2012), our data suggest that modest elevations, similar to those proposed in the northern Sierra Nevada (Hren et al., 2010; Mix et al., 2016), extended relatively far south in the early Eocene.

CONCLUSIONS

We found evidence for cool water temperatures and isotopically light freshwater in the early Eocene of southern California using clumped and triple oxygen isotopes in oyster shells. Cool Δ_{47} temperatures measured in the sea-level oyster shells ($9\text{--}20^\circ\text{C}$) challenge the idea of invariably high temperatures during hothouse climates. We found low $\Delta^{17}\text{O}$ values in oyster shells that indicate highly evaporated freshwater and/or mixing between freshwater

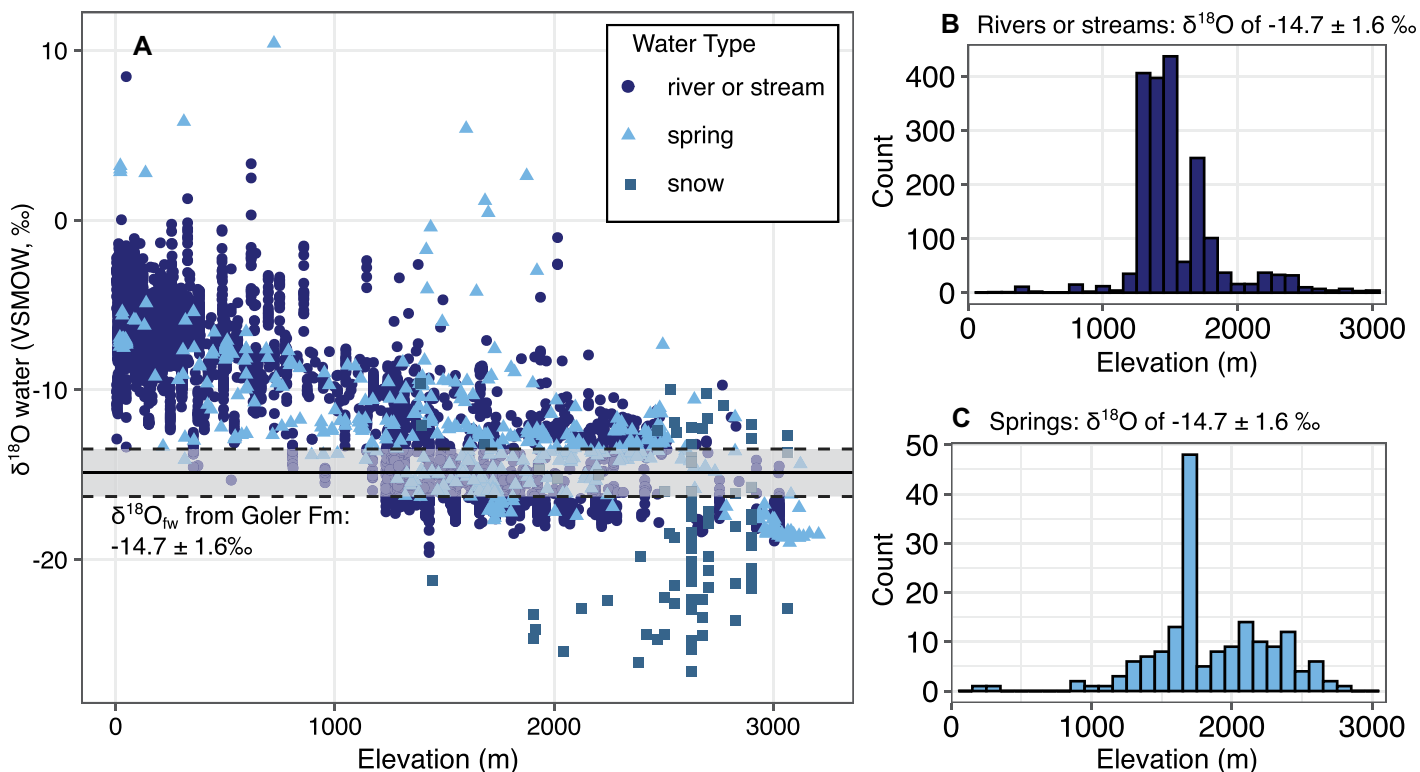


Figure 3. Modern water isotope data from latitudes within 5° of the Goler Formation (between 31°N and 41°N) in North America (published values are reported in the WaterIsotopes Database [<https://wateriso.utah.edu/waterisotopes/>]; see the Supplemental Material [see footnote 1]). (A) Elevation- $\delta^{18}\text{O}$ relationship for modern rivers, springs, and snow. (B,C) Elevation distributions for rivers/streams and springs with $\delta^{18}\text{O}$ between -16.3‰ and -13.1‰ (i.e., $-14.7\text{‰} \pm 1.6\text{‰}$, minimum $\delta^{18}\text{O}_{\text{fw}}$ value from Goler Formation shells).

and ocean water in an estuary. In the favored estuarine explanation, we estimated a minimum $\delta^{18}\text{O}_{\text{fw}}$ value of $-14.7\text{\textperthousand} \pm 1.6\text{\textperthousand}$. Taking our minimum estimate of $\delta^{18}\text{O}_{\text{fw}}$, the Goler estuary was likely fed by waters sourced from moderate elevations (>1 km), consistent with previous estimates of a Nevadaplano at ~ 2 – 3 km in elevation at that time. Without $\Delta^{17}\text{O}$, we would have estimated a freshwater $\delta^{18}\text{O}$ value of $-9\text{\textperthousand}$, leading to an underestimate of upstream elevations. To our knowledge, this is the first method that allows for independent estimation of $\delta^{18}\text{O}_{\text{fw}}$ in an estuary. Our findings highlight the potential for clumped and triple oxygen isotope analyses to enhance reconstructions of $\delta^{18}\text{O}$ values of meteoric waters, which are critical for understanding hydroclimate and elevations in geologic time.

ACKNOWLEDGMENTS

Oyster shells from the Goler Formation were provided by D. Lofgren from collections at the Raymond Alf Museum. R. Mulcrone assisted in collecting modern mollusk shells. T. Huth, D. Yarian, K. Lohmann, and L. Wingate assisted with analyses. Funding came from U.S. National Science Foundation grant EAR-PF 1854873 to J.R. Kelson and grant OCE-PF 1420902 to S.V. Petersen.

REFERENCES CITED

- Albright, L.B., Lofgren, D.L., and McKenna, M.C., 2010, Magnetostratigraphy, mammalian biostratigraphy, and refined age assessment of the Goler Formation (Paleocene), California: Papers on Geology, Vertebrate Paleontology, and Biostratigraphy in Honor of Michael O. Woodburne: Museum of Northern Arizona Bulletin, v. 65, p. 259–279.
- Aron, P.G., Levin, N.E., Beverly, E.J., Huth, T.E., Passey, B.H., Pelletier, E.M., Poulsen, C.J., Winkelstern, I.Z., and Yarian, D.A., 2021, Triple oxygen isotopes in the water cycle: Chemical Geology, v. 565, p. 120026, <https://doi.org/10.1016/j.chemgeo.2020.120026>.
- Barkan, E., and Luz, B., 2007, Diffusivity fractions of $\text{H}_2^{16}\text{O}/\text{H}_2^{17}\text{O}$ and $\text{H}_2^{16}\text{O}/\text{H}_2^{18}\text{O}$ in air and their implications for isotope hydrology: Rapid Communications in Mass Spectrometry, v. 21, p. 2999–3005, <https://doi.org/10.1002/rctm.3180>.
- Chapman, A.D., Saleeby, J.B., Wood, D.J., Piasecki, A., Kidder, S., Ducea, M.N., and Farley, K.A., 2012, Late Cretaceous gravitational collapse of the southern Sierra Nevada batholith, California: Geosphere, v. 8, p. 314–341, <https://doi.org/10.1130/GES00740.1>.
- Cox, B.F., 1982, Stratigraphy, Sedimentology, and Structure of the Goler Formation (Paleocene), El Paso Mountains, California: Implications for Paleogene Tectonism on the Garlock Fault Zone [Ph.D. thesis]: Riverside, California, University of California–Riverside, 300 p.
- Fan, M., and Dettman, D.L., 2009, Late Paleocene high Laramide ranges in northeast Wyoming: Oxygen isotope study of ancient river water: Earth and Planetary Science Letters, v. 286, p. 110–121, <https://doi.org/10.1016/j.epsl.2009.06.024>.
- Hemingway, J.D., and Henkes, G.A., 2021, A disordered kinetic model for clumped isotope bond reordering in carbonates: Earth and Planetary Science Letters, v. 566, 116962, <https://doi.org/10.1016/j.epsl.2021.116962>, corrigendum available at <https://doi.org/10.1016/j.epsl.2021.117191>.
- Hollis, C.J., et al., 2019, The DeepMIP contribution to PMIP4: Methodologies for selection, compilation and analysis of latest Paleocene and early Eocene climate proxy data, incorporating version 0.1 of the DeepMIP database: Geoscientific Model Development Discussions, v. 12, p. 1–98, <https://doi.org/10.5194/gmd-2018-309>.
- House, M.A., Wernicke, B.P., and Farley, K.A., 1998, Dating topography of the Sierra Nevada, California, using apatite (U-Th)/He ages: Nature, v. 396, p. 66–69, <https://doi.org/10.1038/23926>.
- Hren, M.T., Pagani, M., Erwin, D.M., and Brandon, M.T., 2010, Biomarker reconstruction of the early Eocene paleotopography and paleoclimate of the northern Sierra Nevada: Geology, v. 38, p. 7–10, <https://doi.org/10.1130/G30215.1>.
- Huth, T.E., Passey, B.H., Cole, J.E., Lachniet, M.S., McGee, D., Denniston, R.F., Truebe, S., and Levin, N.E., 2022, A framework for triple oxygen isotopes in speleothem paleoclimatology: Geochimica et Cosmochimica Acta, v. 319, p. 191–219, <https://doi.org/10.1016/j.gca.2021.11.002>.
- Ibarra, D.E., Kukla, T., Methner, K.A., Mulch, A., and Chamberlain, C.P., 2021, Reconstructing past elevations from triple oxygen isotopes of lacustrine chert: Application to the Eocene Nevadaplano, Elko Basin, Nevada, United States: Frontiers of Earth Science, v. 9, 628868, <https://doi.org/10.3389/feart.2021.628868>.
- Kim, S.-T., and O’Neil, J.R., 1997, Equilibrium and nonequilibrium oxygen isotope effects in synthetic carbonates: Geochimica et Cosmochimica Acta, v. 61, p. 3461–3475, [https://doi.org/10.1016/S0016-7037\(97\)00169-5](https://doi.org/10.1016/S0016-7037(97)00169-5).
- Lechner, A.R., and Niemi, N.A., 2011, Sedimentologic and isotopic constraints on the Paleogene paleogeography and paleotopography of the southern Sierra Nevada, California: Geology, v. 39, p. 379–382, <https://doi.org/10.1130/G31535.1>.
- Lechner, A.R., Niemi, N.A., Hren, M.T., and Lohmann, K.C., 2013, Paleoelevation estimates for the northern and central proto-Basin and Range from carbonate clumped isotope thermometry: Tectonics, v. 32, p. 295–316, <https://doi.org/10.1002/tect.20016>.
- Lofgren, D., McKenna, M., Honey, J., Nydam, R., Wheaton, C., Yokote, B., Henn, L., Hanlon, W., Manning, S., and McGee, C., 2014, New records of eutherian mammals from the Goler Formation (Tiffanian, Paleocene) of California and their biostratigraphic and paleobiogeographic implications: American Museum Novitates, v. 3797, p. 1–57, <https://doi.org/10.1206/3797.1>.
- Lunt, D.J., et al., 2021, DeepMIP: Model intercomparison of early Eocene climatic optimum (EECO) large-scale climate features and comparison with proxy data: Climate of the Past, v. 17, p. 203–227, <https://doi.org/10.5194/cp-17-203-2021>.
- Luz, B., and Barkan, E., 2010, Variations of $^{17}\text{O}/^{16}\text{O}$ and $^{18}\text{O}/^{16}\text{O}$ in meteoric waters: Geochimica et Cosmochimica Acta, v. 74, p. 6276–6286, <https://doi.org/10.1016/j.gca.2010.08.016>.
- Macarewicz, S.I., Poulsen, C.J., and Montañez, I.P., 2021, Simulation of oxygen isotopes and circulation in a late Carboniferous epicontinental sea with implications for proxy records: Earth and Planetary Science Letters, v. 559, 116770, <https://doi.org/10.1016/j.epsl.2021.116770>.
- McDougall, K., 1987, Foraminiferal biostratigraphy and paleoecology of marine deposits, Goler Formation, California, in Cox, B.F., ed., Basin Analysis and Paleontology of the Paleocene and Eocene Goler Formation, El Paso Mountains, California: Pacific Section, Society of Economic Paleontologists and Mineralogists (SEPM) Special Publication 57, p. 43–67.
- Mix, H.T., Ibarra, D.E., Mulch, A., Graham, S.A., and Chamberlain, C.P., 2016, A hot and high Eocene Sierra Nevada: Geological Society of America Bulletin, v. 128, p. 531–542, <https://doi.org/10.1130/B31294.1>.
- Naafs, B.D.A., et al., 2018, High temperatures in the terrestrial mid-latitudes during the early Palaeogene: Nature Geoscience, v. 11, p. 766–771, <https://doi.org/10.1038/s41561-018-0199-0>.
- Passey, B.H., and Ji, H., 2019, Triple oxygen isotope signatures of evaporation in lake waters and carbonates: A case study from the western United States: Earth and Planetary Science Letters, v. 518, p. 1–12, <https://doi.org/10.1016/j.epsl.2019.04.026>.
- Passey, B.H., Hu, H., Ji, H., Montanari, S., Li, S., Henkes, G.A., and Levin, N.E., 2014, Triple oxygen isotopes in biogenic and sedimentary carbonates: Geochimica et Cosmochimica Acta, v. 141, p. 1–25, <https://doi.org/10.1016/j.gca.2014.06.006>.
- Petersen, S.V., et al., 2019, Effects of improved ^{17}O correction on interlaboratory agreement in clumped isotope calibrations, estimates of mineral-specific offsets, and temperature dependence of acid digestion fractionation: Geochimistry Geophysics Geosystems, v. 20, p. 3495–3519, <https://doi.org/10.1029/2018GC008127>.
- Petersen, S.V., Tabor, C.R., Lohmann, K.C., Poulsen, C.J., Meyer, K.W., Carpenter, S.J., Erickson, J.M., Matsunaga, K.K.S., Smith, S.Y., and Sheldon, N.D., 2016, Temperature and salinity of the Late Cretaceous Western Interior Seaway: Geology, v. 44, p. 903–906, <https://doi.org/10.1130/G38311.1>.
- Rowley, D.B., 2007, Stable isotope-based paleoaltimetry: Theory and validation: Reviews in Mineralogy and Geochemistry, v. 66, p. 23–52, <https://doi.org/10.2138/rmg.2007.66.2>.
- Sackett, W.M., and Moore, W.S., 1966, Isotopic variations of dissolved inorganic carbon: Chemical Geology, v. 1, p. 323–328, [https://doi.org/10.1016/0009-2541\(66\)90028-3](https://doi.org/10.1016/0009-2541(66)90028-3).
- Snell, K.E., Koch, P.L., Druschke, P., Foreman, B.Z., and Eiler, J.M., 2014, High elevation of the ‘Nevadaplano’ during the Late Cretaceous: Earth and Planetary Science Letters, v. 386, p. 52–63, <https://doi.org/10.1016/j.epsl.2013.10.046>.
- Squires, R.L., 2018, Paleocene and Eocene oysters from the West Coast of the United States: Revision of named species and recognition of new species: Contributions in Science, v. 526, p. 1–29, <https://doi.org/10.5962/p.320145>.
- Surge, D., Lohmann, K.C., and Dettman, D.L., 2001, Controls on isotopic chemistry of the American oyster, *Crassostrea virginica*: Implications for growth patterns: Palaeogeography, Palaeoclimatology, Palaeoecology, v. 172, p. 283–296, [https://doi.org/10.1016/S0031-0182\(01\)00303-0](https://doi.org/10.1016/S0031-0182(01)00303-0).
- Veizer, J., et al., 1999, $^{87}\text{Sr}/^{86}\text{Sr}$, ^{13}C and ^{18}O evolution of Phanerozoic seawater: Chemical Geology, v. 161, p. 59–88, [https://doi.org/10.1016/S0009-2541\(99\)00081-9](https://doi.org/10.1016/S0009-2541(99)00081-9).
- Wostbrock, J.A.G., Cano, E.J., and Sharp, Z.D., 2020, An internally consistent triple oxygen isotope calibration of standards for silicates, carbonates and air relative to VSMOW2 and SLAP2: Chemical Geology, v. 533, 119432, <https://doi.org/10.1016/j.chemgeo.2019.119432>.
- Yapp, C.J., 2008, $^{18}\text{O}/^{16}\text{O}$ and D/H in goethite from a North American Oxisol of the early Eocene climatic optimum: Geochimica et Cosmochimica Acta, v. 72, p. 5838–5851, <https://doi.org/10.1016/j.gca.2008.09.002>.
- Zhu, J., Poulsen, C.J., and Tierney, J.E., 2019, Simulation of Eocene extreme warmth and high climate sensitivity through cloud feedbacks: Science Advances, v. 5, eaax1874, <https://doi.org/10.1126/sciadv.aax1874>.

Printed in USA